Title
Bilayer silk fibroin grafts support functional oesophageal repair in a rodent model of caustic injury

Journal
Journal of Tissue Engineering and Regenerative Medicine, 12(2)

ISSN
1932-6254

Authors
Algarrahi, Khalid
Franck, Debra
Savarino, Alyssa
et al.

Publication Date
2018-02-01

DOI
10.1002/term.2434

Peer reviewed

HHS Public Access

Author manuscript

J Tissue Eng Regen Med. Author manuscript; available in PMC 2019 February 01.

Published in final edited form as:

J Tissue Eng Regen Med. 2018 February ; 12(2): e1068–e1075. doi:10.1002/term.2434.

Bi-layer Silk Fibroin Grafts Support Functional Esophageal Repair in a Rodent Model of Caustic Injury

Khalid Algarrahi[1,2], **Debra Franck**[1], **Alyssa Savarino**[1], **Vivian Cristofaro**[2,3,4], **Xuehui Yang**[1], **Saif Affas**[1,2], **Frank-Mattias Schäfer**[1], **Maryrose P. Sullivan**[2,3,4], **Carlos R. Estrada Jr**[1,2], and **Joshua R. Mauney**[1,2,§]

[1]Urological Diseases Research Center, Boston Children's Hospital, Boston, MA 02115, USA

[2]Department of Surgery, Harvard Medical School, Boston, MA 02115, USA

[3]Division of Urology, Veterans Affairs Boston Healthcare System, West Roxbury, MA 02132, USA

[4]Department of Surgery, Brigham and Women's Hospital, Boston, MA 02115, USA

Abstract

Surgical repair of caustic esophageal injuries with autologous gastrointestinal segments is often associated with dysmotility, dysphagia, and donor site morbidity and therefore alternative graft options are needed. Bi-layer silk fibroin (BLSF) scaffolds were assessed for their ability to support functional restoration of damaged esophageal tissues in a rat model of onlay esophagoplasty. Transient exposure of isolated esophageal segments with 40% NaOH led to corrosive esophagitis and a 91% reduction in the luminal cross-sectional area of damaged sites. Esophageal repair with BLSF matrices was performed in injured rats (N=27) as well as a nondiseased cohort (N=12) for up to 2 m of implantation. Both implant groups exhibited >80% survival rates, displayed similar degrees of weight gain, and were capable of solid food consumption following a 3 d liquid diet. End-point μ-computed tomography of repaired sites demonstrated a 4.5-fold increase in luminal cross-sectional area over baseline injury levels. Reconstructed esophageal conduits from damaged and nondiseased animals produced comparable contractile responses to KCl and electric field stimulation while isoproterenol generated similar tissue relaxation responses. Histological and immunohistochemical evaluations of neotissues from both implant groups showed formation of a stratified, squamous epithelium with robust cytokeratin expression as well as skeletal and smooth muscle layers positive for contractile protein expression. In addition, synaptophysin positive neuronal junctions and vessels lined with CD31 positive endothelial cells were also observed at graft sites in each setting. These results provide preclinical validation for the use of BLSF scaffolds in reconstructive strategies for esophageal repair following caustic injury.

[§]Corresponding author: Joshua R. Mauney, Ph.D., Boston Children's Hospital, Department of Urology, John F. Enders Research Laboratories, 300 Longwood Ave., Rm. 1009, Boston, MA 02115, USA; Phone: 617-919-2521; Fax: 617-730-0248; joshua.mauney@childrens.harvard.edu.

Conflict of interest

The authors declare no conflicts of interest.

Author Contributions

JRM and KA designed and conceptualized this study. Acquisition of data was carried out by KA, DF, VC, XY, AS, SA, FMS and MPS. Analysis and interpretation of data was done by JRM, KA, DF, VC, AS, and MPS. Manuscript was drafted by JRM, KA, VC, MPS, while VC, MPS, CRE, and JRM performed critical revision of the manuscript for important intellectual content. Statistical analysis was done by KA, VC, and MPS. Funding was obtained by JRM and CRE. The entire study was supervised by JRM.

1. Introduction

Accidental ingestion of caustic alkali agents is highly prevalent in the worldwide pediatric population and frequently results in corrosive esophagitis, stenosis, and ultimately esophageal stricture formation (Uygun, 2015). Endoscopic balloon dilatation and the use of temporary stents represent the primary treatment options for increasing luminal esophageal caliber while also improving dysphagia symptoms associated with caustic injury (Dall'Oglio *et al.,* 2016). Unfortunately, dilatation of the esophagus carries the risk of organ perforation and over time this pathology can become refractory to this approach (Ramareddy and Alladi 2016). Similarly, stent-related complications such as device migration and erosion are significant concerns for this mode of therapy (Zhao *et al.,* 2016). In patients where conventional management fails, gastric transposition and colonic interposition grafts are used to replace diseased esophageal segments (Ezemba *et al.,* 2014). However, these procedures can lead to severe adverse events such as esophageal dysmotility, anastomotic leakage, and donor site morbidity, all of which can negatively impact patient quality of life (Reinberg, 2016). Matrices derived from decellularized tissues or synthetic polymers have been previously investigated as alternatives to autologous gastrointestinal segments in both animal models and clinical settings of esophageal reconstruction (Badylak *et al.,* 2000, 2011; Aikawa *et al.,* 2013; Dua *et al.,* 2016). Suboptimal outcomes with these scaffold configurations including implant contracture, graft perforation, and stenosis have been reported (Lopes *et al.*,2006;Doede *et al.,* 2009; Badylak *et al.,* 2011), thus emphasizing the need to explore new biomaterials for esophageal repair.

Bi-layer silk fibroin (BLSF) grafts represent emerging, biodegradable platforms for esophageal tissue engineering. The multi-functional implant design promotes initial defect consolidation and preservation of organ continuity via a fluid-tight film layer, whereas a porous foam compartment serves as a conduit for host tissue integration (Seth *et al.,* 2013; Algarrahi *et al.,* 2015). A recent report from our laboratory has demonstrated the feasibility of these matrices for onlay esophagoplasty in a nondiseased, rodent model of acute traumatic injury (Algarrahi *et al.,* 2015). In this system, BLSF scaffolds promoted constructive remodeling of esophageal defects with neotissues capable of supporting peristalsis and solid food consumption (Algarrahi *et al.,* 2015). Parallel comparisons with conventional small intestinal submucosa (SIS) grafts revealed BLSF matrices achieved significantly higher degrees of skeletal muscle formation, de novo innervation, as well as reduced inflammatory reactions within implantation sites (Algarrahi *et al.,* 2015).

Although the initial performance of BLSF scaffolds for esophageal repair was encouraging, the use of nondiseased animal models may not accurately predict graft performance in patients with underlying pathologies due to alterations in the regenerative capacity of host tissues. For instance, Akbal and colleagues reported that while augmentation of healthy porcine bladders with an acellular dermal biomatrix resulted in excellent functional bladder tissue regeneration, similar experiments in a porcine model of obstructed bladder disease failed to show favorable results (Akbal *et al.,* 2006). Moreover, onlay urethroplasty of damaged rabbit urethras with SIS grafts revealed delayed epithelialization and abnormal distribution of smooth muscle tissue in comparison to the outcomes achieved in healthy

animals (Villoldo *et al.,* 2013). Therefore the objective of this study in rats was to establish whether BLSF scaffolds have the same regenerative capacity when onlay esophagoplasty is performed following caustic injury in comparison to a nondiseased setting.

2. Materials and Methods

2.1. Biomaterials

BLSF scaffolds were fabricated from *Bombyx mori* silkworm cocoons using a solvent-casting/salt leaching process in combination with silk fibroin film casting as previously reported (Seth *et al.,* 2013). The structural and tensile properties of the graft have been reported in published studies (Seth *et al.*, 2013). Matrices were sterilized in 70% ethanol and rinsed in phosphate buffered saline (PBS) prior to surgical procedures.

2.2. Surgical procedures

All animal studies were approved by the Boston Children's Hospital Animal Care and Use Committee prior to experimentation and performed under protocol 16-05-3161R.

Caustic esophageal injury was induced in female Sprague-Dawley rats (N=68, 6–8 wks of age, ~250–300 g, Charles River Laboratories, Wilmington, MA) using a NaOH burn model described by Okata and colleagues (Okata *et al.,* 2011) with some modifications. Prior to surgery, rats were maintained for a maximum of 24 h on a liquid diet consisting of a nutritionally-balanced commercial formula (TestDiet®, Richmond, IN mixed with PediaSure®, Abbott Laboratories, Columbus, OH) and were given ready access to water. Under general anesthesia induced by isoflurane inhalation, rats were placed in a supine position with the thorax elevated to 30 degrees. An upper midline laparotomy incision was made through the skin and underlying rectus muscle in a sterile fashion in order to isolate a 1 cm segment of the abdominal esophagus. A 5 French double lumen Vascu-PICC line (Medcomp®, Harleysville, PA) was placed in the upper part of the abdominal esophagus via the mouth and vessel loops (DevonTM, Mansfield, MA) were tied externally around the gastroesophageal junction and 5 mm proximal to compartmentalize NaOH exposure. Catheter infusion of a 40% NaOH solution was performed into the isolated esophageal segment with a total contact time of 2 min which was followed by irrigation with distilled water and subsequent fluid aspiration. The catheter and vessel loops were then removed and non-absorbable 7-0 polypropylene sutures with 4-0 steel rings were positioned at the proximal/distal boundaries of the injured segment for region identification during imaging analyses described below. Following these procedures, the esophagus was replaced into the abdominal cavity. The skin and abdominal incisions were sutured closed. Post-operative pain was managed with subcutaneous injection of 1 mg/kg meloxicam and 0.1 mg/kg buprenorphine. Rats were maintained on liquid diet and imaging evaluations were performed 2 d post-injury to evaluate luminal esophageal caliber. Animals were then either harvested for 2 d post-injury analyses (N=20), subjected to scaffold implantation (N=27) as detailed below, or maintained without surgical intervention (N=5).

Onlay esophagoplasty with BLSF scaffolds was performed as previously described (Algarrahi *et al.,* 2015) in rats at 3 d post-injury. In parallel, a cohort of nondiseased rats

(N=12) were subjected to esophageal reconstruction with BLSF grafts. In both experimental groups, an upper midline laparotomy incision was sterilely performed under isoflurane anesthesia to expose the abdominal esophagus. A 7 × 3 mm^2 elliptical defect was created in the anterior esophageal wall 5 mm above the gastroesophageal junction via surgical tissue resection. An elliptical graft of equal size was anastomosed into the defect site using interrupted 7-0 polyglactin sutures. Non-absorbable 7-0 polypropylene sutures were placed at the proximal/distal and lateral edges of the graft perimeter for identification of graft borders. The esophagus was then returned to the abdominal cavity and incisions were sutured closed. Post-operative pain was managed as described above and rats were maintained on the aforementioned liquid diet for 3 d post-op and subsequently nourished with standard rat feed for the study duration. Animals were weighed prior to surgery and every week until scheduled euthanasia. Rats subjected to caustic injury and implanted with BLSF scaffolds were harvested for endpoint evaluations at 1 wk (N=5), 1 m (N=5), and 2 m (N=17) post-repair. All nondiseased animals grafted with BLSF scaffolds were harvested at 2 m post-implantation for comparative analyses. An additional group of non-surgical, healthy animals (N=12) were evaluated in parallel as positive controls.

2.3. Micro-computed tomography (μ-CT)

μ-CT analysis was performed on experimental groups following contrast agent gavage as previously described (Algarrahi *et al.,* 2015). Luminal esophageal cross-sectional areas (N=7 animals per group) were quantified from the central regions of the original caustic injury sites 2 d following NaOH administration, scaffold implantation sites from damaged and nondiseased cohorts 2 m post-repair, as well as internal noninjured reference points adjacent to the 7th thoracic vertebra (T7) using published methods (Algarrahi *et al.,* 2015). Parallel measurements were executed in corresponding esophageal regions in nonsurgical controls.

2.4. Ex vivo contraction and relaxation responses

Circular esophageal tissues with intact mucosa (N=5 animals per group) were isolated from injured sites 2 d after NaOH exposure, repaired segments from nondiseased and diseased groups at 2 m post-op, as well as nonsurgical controls. Specimens were mounted in tissue baths for isometric tension studies as previously described (Algarrahi *et al.,* 2015). Briefly, contractile responses to KCl (80 mM) and electrical field stimulation (EFS, 25-20 Hz, 0.5 ms pulse duration, 40 volts, 10 s) were measured. In parallel, specimens were pre-contracted with carbachol (3 μM) and relaxation responses were quantified following administration of isoproterenol (10 μM). Contractile responses were expressed as force (mN) normalized by tissue cross-sectional area. Relaxation responses were expressed as percent change from pre-contraction response.

2.5. Histological, immunohistochemical, and histomorphometric analyses

Following animal harvest, tubular esophageal specimens isolated from experimental groups were formalin-fixed, dehydrated in graded alcohols, and paraffin embedded. Sections (5 μm) were stained with Masson's trichrome (MTS) using standard methods. Parallel specimens were analyzed for IHC assessments using primary antibodies to the following markers as previously described (Algarrahi *et al.,* 2015): fast myosin skeletal heavy chain (MYH), α-smooth muscle actin (α-SMA), pan-cytokeratin (CK), CK4, CK14, filaggrin, synaptophysin

(SYP), and CD31. In addition, host tissue responses were evaluated with the following primary antibodies: anti-myeloperoxidase (MPO, Abcam, Cambridge, MA, 1:100 dilution) and anti-CD68 (Thermo Fisher Scientific, Cambridge, MA, 1:200 dilution). Specimens were then stained with species-matched Alexa Fluor 488, 594, and 647-conjugated secondary antibodies (Thermo Fisher Scientific) while 4', 6-diamidino-2-phenyllindole (DAPI) was used as a nuclear counterstain. An Axioplan-2 microscope (Carl Zeiss MicroImaging, Thornwood, NY) was utilized for sample visualization and representative fields were acquired with Axiovision software (version 4.8).

Histomorphometric evaluations (N=4–7 animals per group) were performed using published methods (Algarrahi *et al.,* 2015). Briefly, image thresholding and area measurements were acquired with ImageJ software (version 1.47) on 4 independent microscopic fields per tissue specimen (20× magnification) in order to calculate the percentage of tissue area stained for MYH, α-SMA, and pan-CK per total tissue area examined. The number of SYP+ boutons were also quantified across 4 independent microscopic fields per tissue sample (20× magnification) employing similar methods and normalized to total tissue area analyzed to determine density of synaptic transmission areas. Vessel density was determined in each tissue sample by normalizing the total number of CD31+ vessels present in 2 independent microscopic fields (5×) per total tissue area examined.

2.6. Statistical analysis

Quantitative measurements were evaluated with the Kruskal-Wallis test in combination with the post-hoc Scheffé's method utilizing SPSS Statistics software v19.0 (http://www.spss.com). All data were expressed as means ± standard deviation unless otherwise indicated. Statistically significant values were defined as $p<0.05$.

3. Results and Discussion

Transient exposure of isolated esophageal segments to alkali injury (Figure 1A) induced liquefactive necrosis resulting in corrosive esophagitis characterized by epithelial sloughing, disruption of the muscularis mucosa and muscularis externa layers, as well as mucosal infiltration of CD68+ macrophages and MPO+ neutrophils (Figure 1B). Rat survival rate by 2 d post-injury was 76% (52/68) and without surgical intervention 100% mortality (5/5) was observed by 1 wk following NaOH exposure with early euthanasia required due to hypersalivation, weight loss, or stridor; symptoms indicative of esophageal dysphagia. μ-CT analysis of surviving animals 2 d post-injury revealed a significant 91% mean reduction in the luminal cross-sectional area of the injured sites in respect to T7 reference levels (Figure 1C, D). Published reports of NaOH ingestion in various rat models have observed a positive correlation between submucosal collagen deposition and a reduction in luminal esophageal cross-sectional area consistent with esophageal stricture formation from excessive extracellular matrix formation during wound healing (Senturk et al., 2010; Okata et al., 2011). However, this trend was not observed in our system potentially due to the difference in post-injury endpoints of 2 d in comparison to 1 m utilized in previous studies (Senturk *et al.,* 2010; Okata *et al.,* 2011). Our data imply acute inflammatory responses following NaOH exposure are the likely mediators of esophageal stenosis detected in the current setting.

Esophageal reconstruction was performed 3 d following caustic burn injury due to the 100% mortality rate observed in animals by 1 wk wherein no surgical intervention was performed.

Prior to scheduled euthanasia, the survival rate of injured rats repaired with BLSF scaffolds was 81% (22/27) with animal death occurring in the initial 5 d post implantation due to esophageal obstruction from fur ingestion (4/5) or peritonitis due to a putative leak at the anastomotic perimeter (1/5). In parallel, nondiseased animals subjected to onlay esophagoplasty demonstrated a 92% survival rate (11/12) with mortality from obstruction secondary to fur ingestion noted in one replicate at 1 m following grafting. None of the surviving rats in either group displayed clinical symptoms of dysphagia over the course of the study period. In addition, both experimental cohorts were capable of solid food consumption after a 3 d liquid diet and exhibited comparable degrees of weight gain by 2 m post-op (Figure 2A). Global tissue evaluations at 2 m post-op of both nondiseased and injured implant groups revealed prominent host tissue ingrowth throughout the original graft sites with no evidence of significant axial contraction between proximal and distal marking sutures (Figure 2B). Endpoint μ-CT evaluations of repaired injury sites revealed preservation of organ continuity with no evidence of anatomical anomalies (Figure 2C). In comparison to baseline levels prior to scaffold implantation, repaired diseased conduits displayed a significant 4.5-fold increase in luminal cross-sectional area which was statistically similar to nonsurgical controls (Figure 2D). These results highlight the ability of BLSF grafts to promote de novo tissue formation and restore function at caustic esophageal injury sites.

Constructive tissue remodeling and host tissue responses were temporally evaluated in damaged esophagi following BLSF matrix implantation by MTS analysis (Figure 3). At 1 wk post-op, a fibrovascular scar populated by mononuclear inflammatory cells as well as myofibroblasts was evident at graft sites and lined by a stratified squamous, keratinized epithelium. The de novo esophageal wall contained residual scaffold fragments with putative sites of macrophage phagocytosis located around the perimeters. Invasion of host skeletal muscle fibers and smooth muscle bundles were localized at the peripheral boundaries of the neotissues. At 1 m post-implantation, an ECM-rich lamina propria had developed and both the de novo muscularis mucosa and muscularis externa had further integrated into the graft region. In addition, organization of the muscularis externa into circular and outer longitudinal skeletal muscle layers was apparent at the edges of the neotissues, however fibrosis still persisted toward internal areas. The de novo muscularis externa at 2 m following repair of injured sites demonstrated a qualitative increase in skeletal muscle density within the central regions of the graft site in comparison to early timepoints. Areas of fibrosis had also diminished at this stage of regeneration and no chronic inflammatory reactions were noted. The structural architecture of neotissues generated in the setting of caustic damage was qualitatively similar to the nondiseased repair group at 2 m post-op. However, maturation of the muscularis mucosa and muscularis externa compartments in both these cohorts was notably underdeveloped in respect to nonsurgical controls. Finally, the temporal stages of wound healing encountered during repair of caustic injury sites with BLSF scaffolds were found to mimic the regenerative responses previously observed in our nondiseased model of esophagoplasty (Algarrahi *et al.,* 2015).

IHC (Figure 4A) and parallel histomorphometric (Figure 4B) evaluations were executed on experimental groups to further characterize the phases of regeneration during repair of damaged regions and compare the degree of tissue maturation achieved between diseased and nondiseased counterparts. Pan-CK+ epithelia were first observed spanning reconstructed injury sites at 1 wk following matrix grafting. By 2 m post-op, no significant differences in the extent of pan-CK+ epithelia were noted between implant groups or nonsurgical controls. In addition, distinct epithelial subpopulations were present in all experimental groups and consisted of CK14+basal cells, polygonal CK4+ suprabasal cells, and flattened FG+ superficial cells. Regenerated vascular networks containing vessels lined with CD31+ endothelial cells were found in both nondiseased and diseased graft sites at all examined timepoints. The mean vessel density was significantly higher in consolidated tissues from all groups in respect to nonsurgical control levels indicating an ongoing stage of tissue remodeling (Zawicki *et al.,* 1981; Jain, 2003). Analysis of de novo innervation revealed synaptic transmission areas marked by SYP+ boutons in all neotissues. There was no significant difference between the densities of SYP+ boutons in implant groups at 2 m post-op compared to nonsurgical control levels. Characterization of the regenerated muscularis externa in neotissues demonstrated the extent of MYH+ skeletal muscle in diseased and nondiseased cohorts had respectively achieved 67% and 76% of control values by 2 m of scaffold implantation. In contrast to other tissue components, animals subjected to caustic injury displayed a reduced capacity to support regeneration of the muscularis mucosa in respect to noninjured subjects. The density of α-SMA+ smooth muscle bundles in this compartment was significantly lower in the diseased setting reflecting 33% of nonsurgical control levels by 2 m post-op, while nondiseased counterparts were capable of supporting 67%. Taken together, these data demonstrate the ability of BLSF grafts to promote the formation of innervated, vascularized esophageal tissues at sites of caustic injury, however the propensity for muscularis mucosal regeneration is muted in comparison to nondiseased microenvironments.

Peristaltic waves generated from radially symmetrical contraction and relaxation of esophageal circular muscle is an essential mechanism for propagation of food bolus through the digestive tract. Contractile behaviors in repaired conduits from each implant group as well as nonsurgical controls and injured segments prior to scaffold implantation were assessed in ex vivo organ bath studies following stimulation with EFS (Figure 5A) and KCl (Figure 5B). In addition, relaxation properties of experimental groups pre-contracted with carbachol were analyzed following isoproterenol treatment (Figure 5C). Alkali injury to esophageal tissues significantly decreased both contractile and relaxation responses to all stimuli tested in comparison to nonsurgical controls. These results are consistent with our histological findings demonstrating extensive caustic damage to esophageal muscular components following transient exposure to NaOH. Following 2 m of BLSF matrix grafting, both repaired nondiseased and diseased conduits demonstrated the ability to contract in response to EFS and KCl stimulation to similar extents. The magnitude of KCl and EFS-induced force generation in these groups was substantially higher than in injured controls, but less than nonsurgical counterparts, suggesting partial recovery of contractile machinery elicited by membrane depolarization as well as neuronal input, respectively. Parallel analysis

of relaxation patterns in experimental groups demonstrated similar trends as observed for contractile responses.

4. Conclusions

The data presented in this study demonstrate the ability of BLSF grafts to promote functional repair of caustic injury sites in a rat model of onlay esophagoplasty. Reconstruction of damaged tissues with BLSF scaffolds restored luminal esophageal caliber, enabled solid food consumption, and promoted the formation of innervated, vascularized epithelial and muscular wall components. In addition, injured esophageal conduits repaired with BLSF grafts displayed contractile and relaxation properties. In comparison to nondiseased settings, BLSF matrices displayed similar regenerative capacities during healing of damaged regions except for a reduced ability to reconstitute the muscularis mucosa to nonsurgical control levels. In summary, these results provide preclinical validation for the potential of BLSF grafts to serve as “off-the-shelf” scaffolds for reconstruction of esophageal tissues following caustic injury.

Acknowledgments

This research was supported by the NIH/NIDDK 1R01DK107568-01A1 (MAUNEY), Tissue Engineering Resource Center, NIH/NIBIB P41 EB002520 (KAPLAN), and BX001790 (MPS). This research was also supported through the vision and generosity of the Rainmaker Group in honor of Dr. Alan Retik, MD. We also acknowledge Dr. Bryan Sack, MD and Mr. Kyle Costa BSc for technical support.

References

Aikawa M, Miyazawa M, Okamoto K, et al. A bioabsorbable polymer patch for the treatment of esophageal defect in a porcine model. J Gastroenterol. 2013; 48:822–829. [PubMed: 23229769]

Akbal C, Lee SD, Packer SC, et al. Bladder augmentation with acellular dermal biomatrix in a diseased animal model. J Urol. 2006; 176:1706–1711. [PubMed: 16945628]

Algarrahi K, Franck D, Ghezzi CE, et al. Acellular bi-layer silk fibroin scaffolds support functional tissue regeneration in a rat model of onlay Esophagoplasty. Biomaterials. 2015; 53:149–159. [PubMed: 25890715]

Badylak SF, Hoppo T, Nieponice A, et al. Esophageal preservation in five male patients after endoscopic inner-layer circumferential resection in the setting of superficial cancer: a regenerative medicine approach with a biologic scaffold. Tissue Eng Part A. 2011; 17:1643–1650. [PubMed: 21306292]

Badylak S, Meurling S, Chen M, et al. Resorbable bioscaffold for esophageal repair in a dog model. J Pediatr Surg. 2000; 35:1097–1103. [PubMed: 10917304]

Dall'Oglio L, Caldaro T, Foschia F, et al. Endoscopic management of esophageal stenosis in children: New and traditional treatments. World J Gastrointest Endosc. 2016; 25:212–219.

Doede T, Bondartschuk M, Joerck C, et al. Unsuccessful alloplastic esophageal replacement with porcine small intestinal submucosa. Artif Organs. 2009; 33:328–333. [PubMed: 19335409]

Dua KS, Hogan WJ, Aadam AA, et al. In-vivo oesophageal regeneration in a human being by use of a non-biological scaffold and extracellular matrix. Lancet. 2016; 388:55–61. [PubMed: 27068836]

Ezemba N, Eze JC, Nwafor IA, et al. Colon interposition graft for corrosive esophageal stricture: midterm functional outcome. World J Surg. 2014; 38:2352–2357. [PubMed: 24748346]

Jain RK. Molecular regulation of vessel maturation. Nat Med. 2003; 9:685–693. [PubMed: 12778167]

Lopes MF, Cabrita A, Ilharco J, et al. Esophageal replacement in rat using porcine intestinal submucosa as a patch or a tube-shaped graft. Dis Esophagus. 2006; 19:254–259. [PubMed: 16866856]

Okata Y, Hisamatsu C, Hasegawa T, et al. Development of a model of benign esophageal stricture in rats: the optimal concentration of sodium hydroxide for stricture formation. Pediatr Surg Int. 2011; 27:73–80. [PubMed: 20865264]

Ramareddy RS, Alladi A. Review of esophageal injuries and stenosis: Lessons learn and current concepts of management. J Indian Assoc Pediatr Surg. 2016; 21:139–143. [PubMed: 27365909]

Reinberg O. Esophageal replacements in children. Ann N Y Acad Sci. 2016; 1381:104–112. [PubMed: 27310521]

Senturk E, Sen S, Pabuccu E, et al. New experimental corrosive esophagitis model in rats. Pediatr Surg Int. 2010; 26:257–261. [PubMed: 20012437]

Seth A, Chung YG, Gil ES, et al. The performance of silk scaffolds in a rat model of augmentation cystoplasty. Biomaterials. 2013; 34:4758–4765. [PubMed: 23545287]

Uygun I. Caustic oesophagitis in children: prevalence, the corrosive agents involved, and management from primary care through to surgery. Curr Opin Otolaryngol Head Neck Surg. 2015; 23:423–432. [PubMed: 26371603]

Villoldo GM, Loresi M, Giudice C, et al. Histologic changes after urethroplasty using small intestinal submucosa unseeded with cells in rabbits with injured urethra. Urology. 2013; 81:1–5. [PubMed: 23200967]

Zawicki DF, Jain RK, Schmid-Schoenbein GW, et al. Dynamics of neovascularization in normal tissue. Microvasc Res. 1981; 21:27–47. [PubMed: 7010086]

Zhao H, Zhou Y, Feng J, et al. Literature Analysis of the Treatment of Benign Esophageal Disease with Stent. Indian J Surg. 2016; 78:6–13. [PubMed: 27186033]

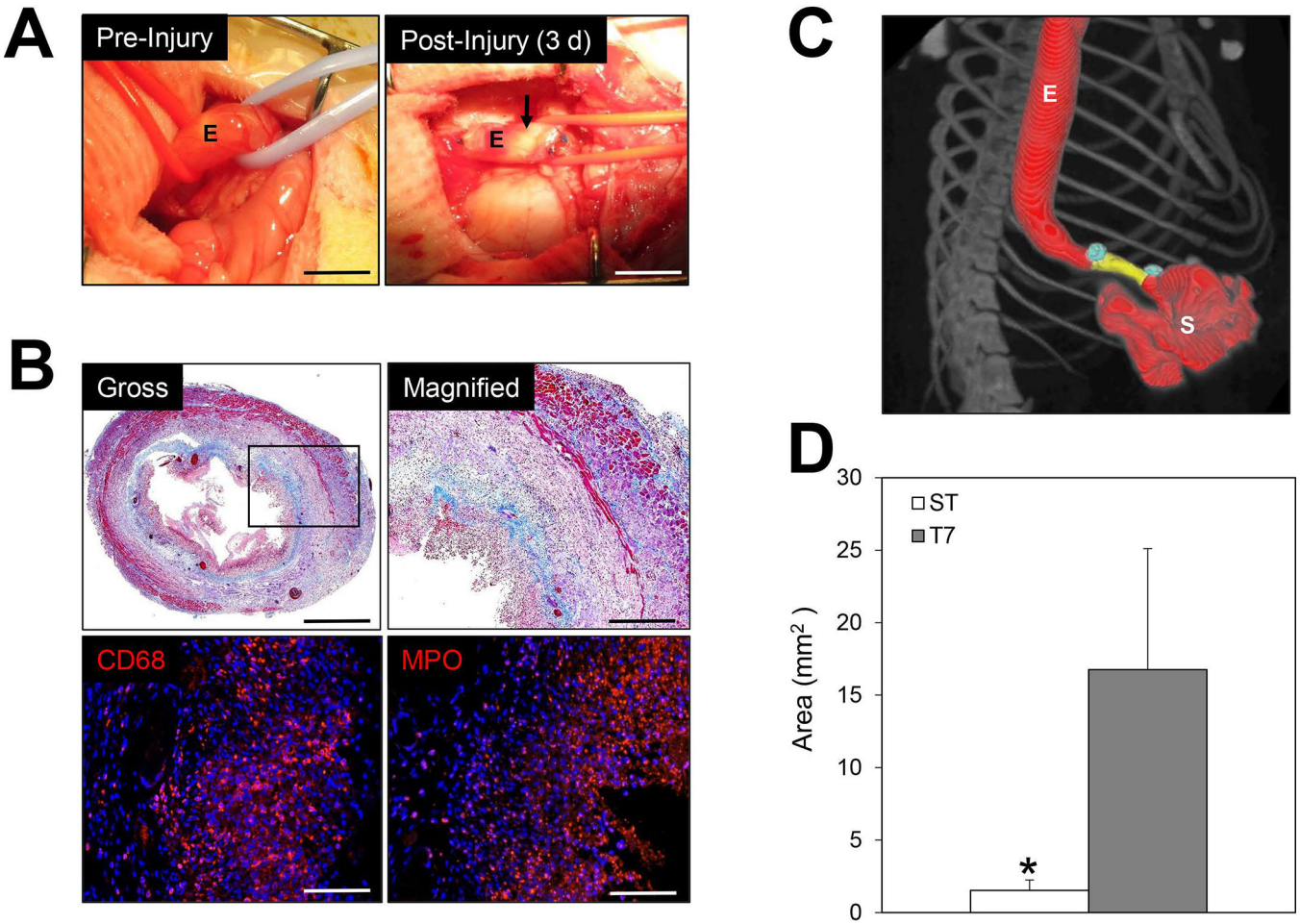

Figure 1.

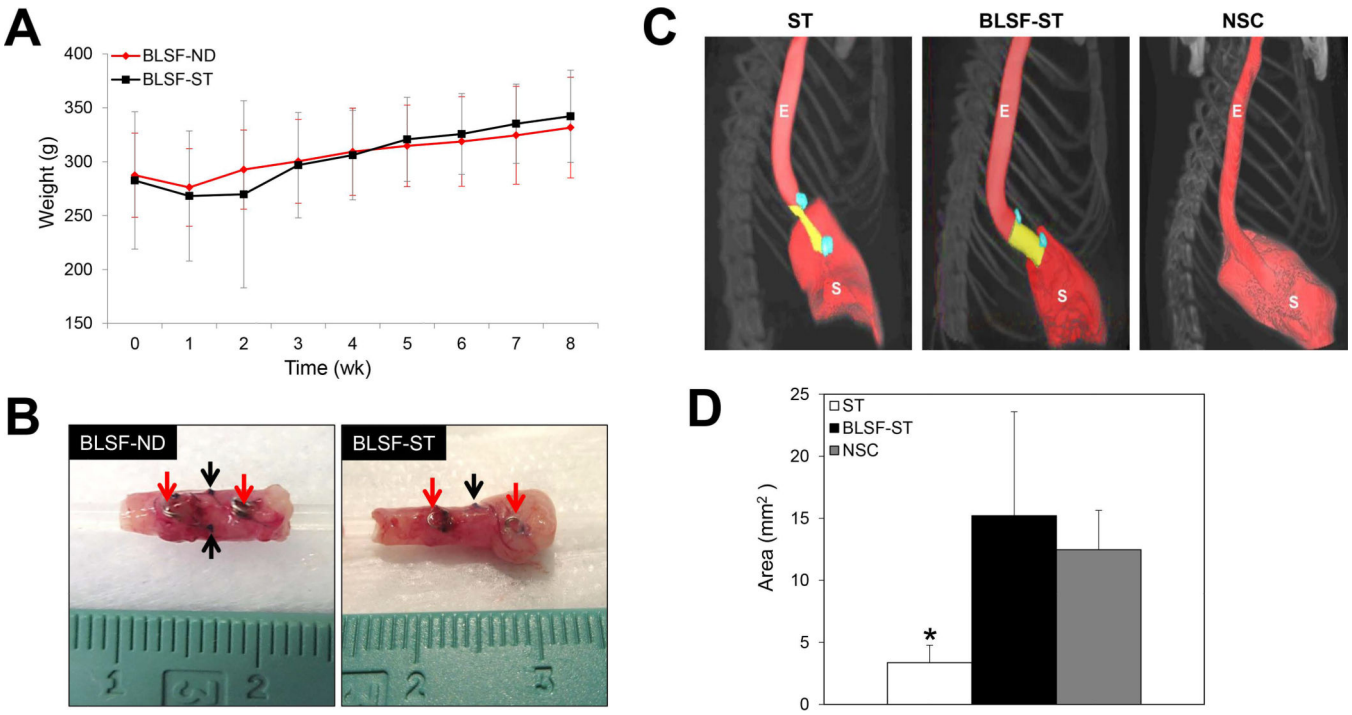

Figure 2.

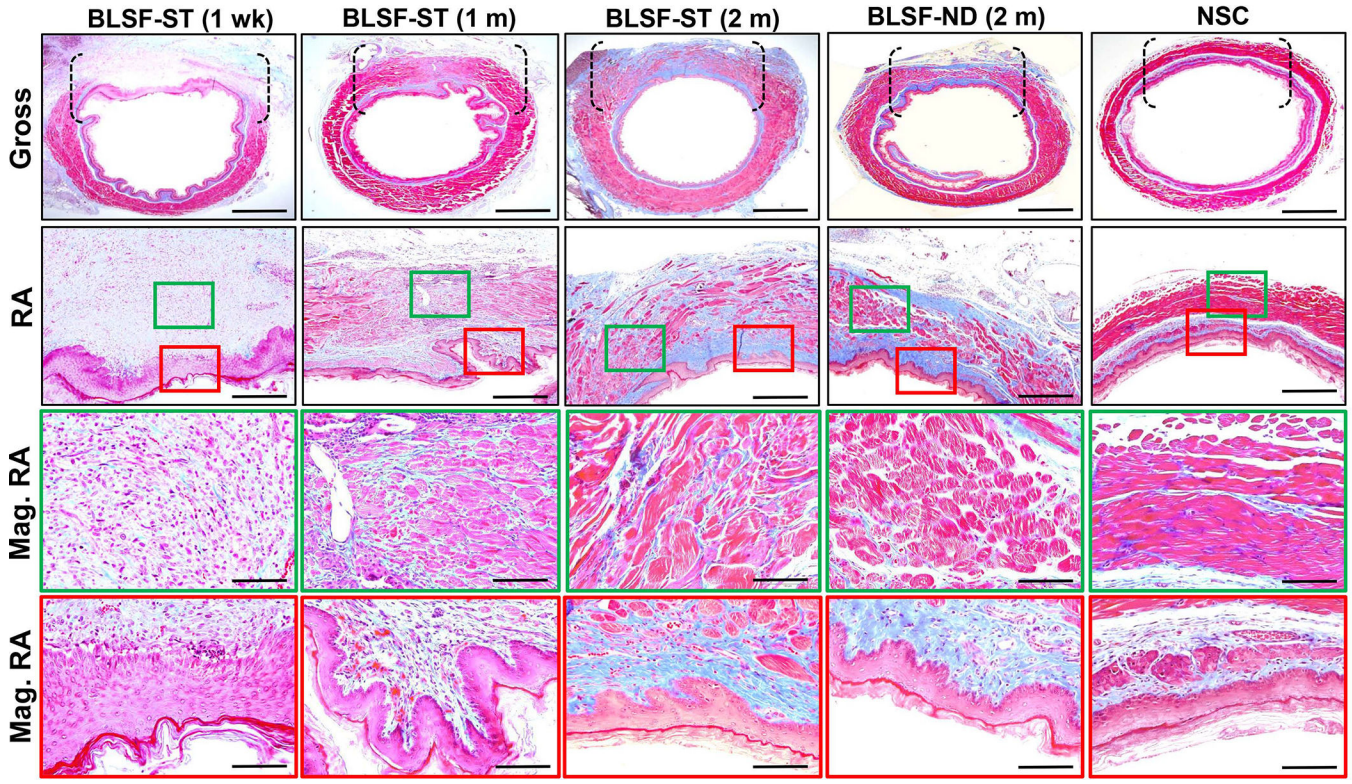

Figure 3.

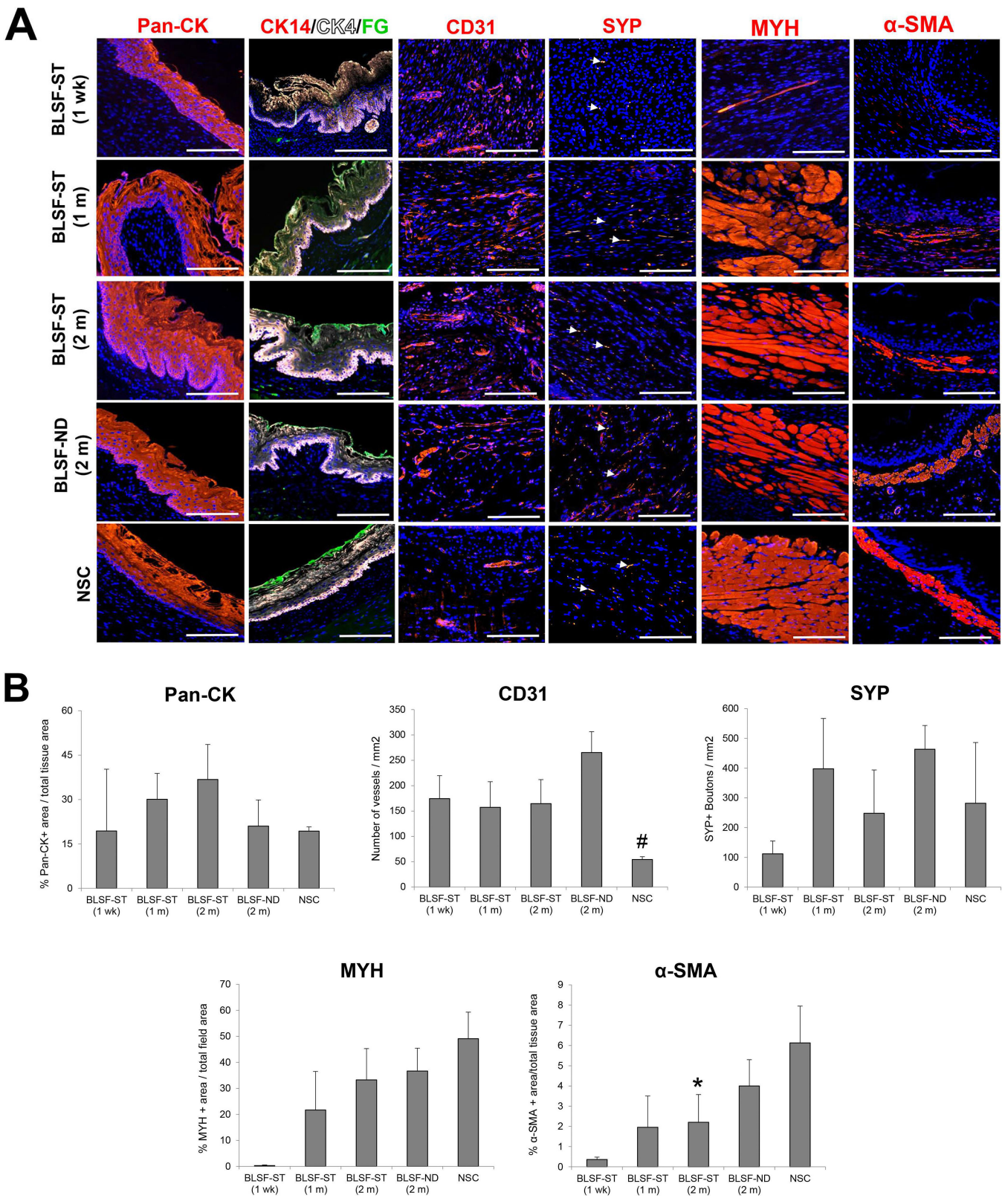

Figure 4.

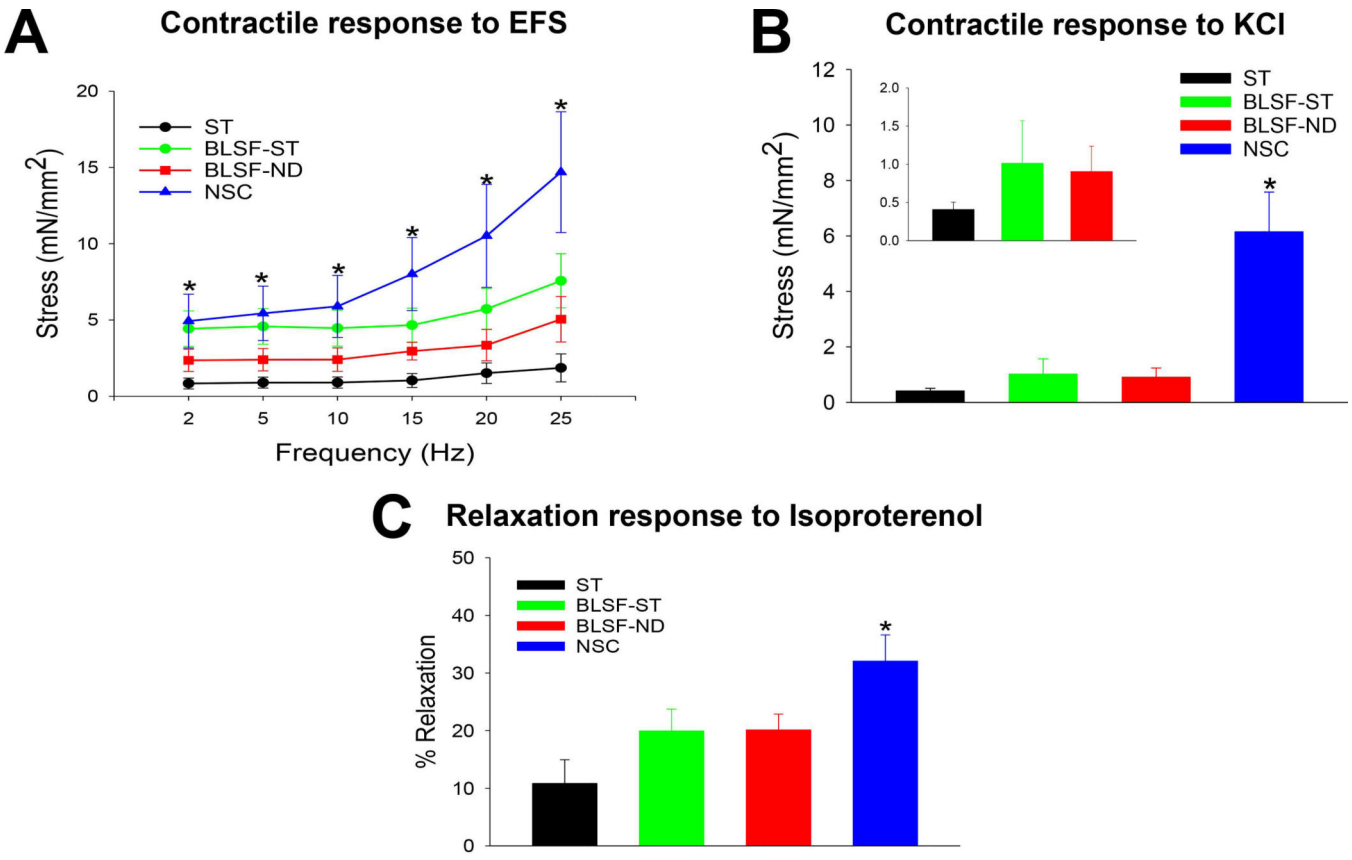

Figure 5.